6th International Conference on Civil Engineering, Architecture and Urban Planning Elites

Berlin, Germany 11-12 Aug 2023

Optimized Values for Lead Core Rubber Bearings for Minimum Response Quantities

Mohammad Reza Bagerzadeh Karimi[1*], Mehmet Cemal Geneş[2]

[1]Cyprus International University, Civil Engineering Department, Nicosia, Cyprus Via Mersin 10, Turkey

[2]Eastern Mediterranean University, Civil Engineering Department, Famagusta, Cyprus via Mersin 10, Turkey

*Corresponding author

Abstract.

In this study, Lead Core Rubber Bearings (LCRB) have been optimized for minimum response quantities by optimizing their mechanical properties under variable pulse-like ground motions, e.g., bearing accelerations and bearing displacements. In order to characterize the general behavior of the base isolation system, random variables have been selected: the isolator period, effective damping ratio, superstructure mass, design displacement, and yield displacement. The shear beam-stick model has been implemented for a single degree seismically-isolated building. Afterward, the dynamic response of the seismic isolation system considering the variability in LCRB and superstructure mass has been investigated. A hysteresis model based on Bouc-Wen is used in the development of the isolation device. The variability of seismic responses has been examined through Monte Carlo simulations (MC). Hence, 37800 time-history analyses were conducted, and the influence of levels of uncertainty of input parameters on seismically isolated buildings' dynamic responses is investigated with 126 natural pulse-like ground motions with pulse periods ranging between 0.6 s and 13 s. Furthermore, the "Desirability Function Optimization" (DFO) method was used to determine the best compound properties of LCRB parameters. Lastly, the LCRB behavior has been optimized as a result of considering uncertainties in the parameters of natural excitation, thereby reducing the response criteria.

Keywords: Monte Carlo simulations, Seismic Isolation System, Desirability Function Optimization, pulse-like ground motions

1. Introduction

Recent publications in structural research have extensively investigated extreme ground motions to safeguard residents' well-being and prevent harm to structures and vibration-sensitive materials. As a result, there has been significant focus on seismic isolation systems in these studies. (Alhan & Öncü-Davas, 2016; Alhan & Gavin, 2005; Bagerzadeh Karimi, 2019; Xu, Chase, & Rodgers, 2014). Seismic isolation is an earthquake-resistant design technique that aims to protect buildings from seismic forces. By incorporating isolators, structures become decoupled from ground movements, leading to reduced forces experienced during earthquakes. This approach enhances the building's performance, allowing it to withstand seismic events more effectively. The popularity of this technique, known as LCRB (Lead Core Rubber Bearing), stems from its cost-effectiveness, practicality, and ease of maintenance, making it widely adopted in earthquake engineering. The Lead Rubber Bearing is composed of alternating layers of rubber and steel sheets, with lead plugs inserted in-between. This configuration allows the lead core to undergo deformation in shear, resulting in bilinear behavior and providing initial stiffness when exposed to low-intensity ground shakes and strong winds. (Tyler & Robinson, 1984). The force-displacement behavior of seismic isolators is influenced by mechanical characteristics that undergo changes throughout the isolator's service life. These characteristics may deviate from their original nominal values, which are determined through prototype tests. Such deviations occur due to various environmental effects and service conditions that the isolator experiences over time (Cheng, Jiang, & Lou, 2008). The variability in mechanical properties caused by these effects necessitates a thorough consideration of isolation system properties for precise analysis and design of seismically isolated structures. Consequently, all structural response parameters should be accounted for, taking into consideration their nominal design values, to ensure the accurate performance and safety of the seismically isolated buildings.

From previous studies, it is evident that the stochastic behavior of base-isolated buildings has been assessed using either synthetically generated ground motions or a limited set of natural ground motions. Additionally, it can be noted that the mechanical properties of the base isolation system showed relatively little variability in these studies. In this current study, the stochastic response of the base isolation system has been evaluated by considering significant variations in the mass of the superstructure and mechanical properties of the base isolation system. These properties include isolator period, effective damping ratio, design displacement, and yielding displacement. Furthermore, special attention has been given to the influence of pulse-like ground motions, which have shown to be highly effective in the analysis (Bagerzadeh Karimi, 2019; Kohrangi, Vamvatsikos, & Bazzurro, 2018; Alhan &

Öncü-Davas, 2016), For this study, a total of 126 natural pulse-like ground motions were selected from the PEER strong ground motion database center. These ground motions were chosen based on their pulse periods, which fall within the range of 0.6 seconds to 13 seconds. A total of 37,800 time-history analyses were carried out for the 126 selected ground motions. In the context of previous research, Monte Carlo (MC) simulation has been recognized as an effective method for obtaining stochastic response statistics. This approach allows for the generation of random samples to simulate the uncertainty and variability in the structural response due to the wide range of ground motion inputs. so, the Monte Carlo (MC) method has been utilized in this study to offer a comprehensive understanding of the variability in seismic responses. The accuracy and precision of the MC simulation depend largely on the number of realizations performed. To achieve the optimal level of precision, the structural model is evaluated using a wide range of input parameters, allowing for a thorough exploration of the system's response under various conditions and uncertainties. This approach helps researchers gain valuable insights into the behavior of the seismically isolated structures and the effects of different input variations on their performance.

2. Structural Seismic mass loading

In this study, the seismic mass of the lumped mass of a one-degree-of-freedom structure has been determined by considering the masses of both a low-rise building (with a fundamental period less than 1 second) and a high-rise building (with a fundamental period higher than 1 second) according to the ASCE/SEI 7-10 guidelines.

To achieve this, two idealized steel structures have been chosen, one with five stories and another with twenty stories, each consisting of six bays in each direction. The plan dimensions of these buildings are illustrated in Figure 1, allowing for a representative analysis of the seismic mass variations based on the building's height and fundamental period. The buildings are designed to have symmetrical square structures with one lateral degree of freedom on each floor. They are modelled as shear-type structures mounted on isolation systems. Each floor's height is 3.4 m, resulting in a total height of 17 m for the 5-storey building and 68 m for the 20-storey building.

Figure 1: Plan of the considered building

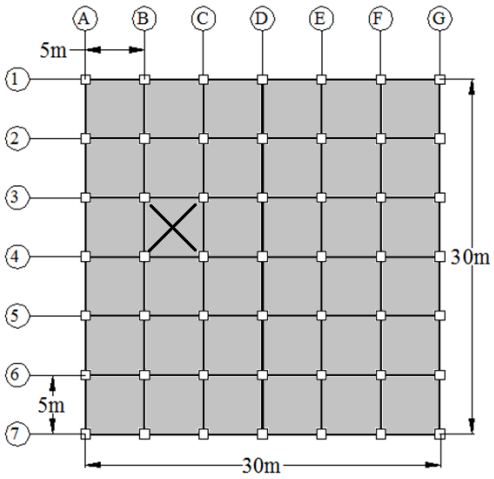

As per Eurocode 8, the total load is defined as "DL+ψ_{2i}LL". In the seismic design load case, the self-weight of each storey, including live and dead loads, is calculated at 8000 N/m^2. The live load is reduced by a factor of $\psi_{2i} = 0.3$. The mass of the roof is determined to be half of the total calculated load. Consequently, the total mass for the conventional 5-storey building is approximately 3240 tons, while the 20-storey building's total mass is estimated to be around 14040 tons. The time history of the benchmark seismically isolated buildings was modelled and analyzed using MATLAB.

3. Uncertain parameters

Uncertain parameters are recognized among a group of input parameters. The behavior of each parameter is defined by a probability measure, such as the Probability Density Function (PDF). To determine the PDF of an uncertain parameter, various sources like experiments, observations, expertise, and experience can be utilized. In situations where there is a lack of experimental data, a standard distribution can be assumed for the uncertain parameter. This study investigates several variables, namely superstructure mass (M), effective damping ratio (β_{eff}), design displacement (D_d), the isolator period (T_{eff}), and yielding displacement (u_y).

The ranges of these variables are shown in Table 1. The value of variable u_y is determined using Eq. (1). Additionally, the mass properties of the superstructure, mounted above the base isolation system, are also treated as variables with values ranging from 3240 to 14040 tons for low-rise (5-storey) and high-rise (20-storey) buildings, respectively. Table 1 provides a visualization of these input uncertain variables related to the mechanical properties of the isolation system and the mass properties of the superstructure, including their mean and standard deviation.

Table 1: Mean, standard deviation, and ranges of uncertain variables

Variable parameters	mean	Standard deviation	Mechanical parameters Ranges
Isolator period ($\mathbf{T_{eff}}$)	4.012 s	0.475 s	$\mathbf{2\ s \le T_{eff} \le 6\ s}$
Damping Ratio ($\boldsymbol{\beta_{eff}}$)	0.100	0.0118	$\mathbf{0.05 \le \beta_{eff} \le 0.15}$
Super structure mass (M)	8612.08 ton	1280.96 ton	$\mathbf{3240\ ton \le M \le 14040\ ton}$
Design displacement ($\mathbf{D_d}$)	72.44 cm	6.544 cm	$\mathbf{45\ cm \le D_d \le 100\ cm}$
Yielding displacement ($\mathbf{u_y = \frac{Q}{k_i - k_p}}$)	1.5 cm	0.246 cm	$\mathbf{0.6\ cm \le u_y \le 3\ cm}$

$$\mathbf{u_y = \frac{Q}{k_i - k_p}} \quad (1)$$

4. Ground motions

Previous research has addressed the significance of pulse-like ground motions and their higher intensity in comparison to non-pulse-like ground motions. The findings suggest that pulse-like records typically lead to amplified structural responses due to spectral enhancements around the pulse period (Kohrangi, Vamvatsikos, & Bazzurro, 2018; Bagerzadeh Karimi, 2019; Elnashai & Sarno, 2008). A collection of 126 pulse-like ground motions has been chosen from the PEER strong ground motions database center. These ground motions encompass a magnitude range from 5 to 8. The supplementary file contains comprehensive data regarding the magnitude and pulse period of each ground motion. Additionally, the file provides supplementary information such as peak ground acceleration (PGA), peak ground velocity (PGV), peak ground displacement (PGD), and earthquake duration for each recorded ground motion.

5. Results and discussion

In this section, the contribution percentage has been determined using the "Analysis of Variance (ANOVA)" tool in Minitab 17 for 37,500 structural responses. To calculate the contribution percentage for each property, the sum of squares term (SS) has been summed across all properties. For each individual SS term, it is divided by the total SS and then multiplied by 100 to obtain the corresponding contribution percentage (Montgomery, 2013).

Hence, Figure 2(A) and Figure 2(B) present the contribution percentage of the mechanical properties of the isolation system (T_{eff}, u_y, D_d and β_{eff}) and ground motion components (T_p, $\frac{PGA}{PGV}$ and $\frac{PGV}{PGD}$) to bearing displacement and acceleration, respectively.

Figure 2(A) indicates that the isolator period contributes the most to bearing displacement, with a percentage of approximately 4.03%, whereas its contribution to bearing acceleration is only about 0.78%. On the other hand, Figure 2(B) demonstrates that the ground motion component with the PGA/PGV ratio significantly influences bearing displacement, accounting for approximately 5.16%,

while its contribution to bearing acceleration is only around 0.29%. The pulse period and the PGV/PGD ratio have minimal contributions to both bearing displacement (approximately 0.01% and 0.2%, respectively) and bearing acceleration. In conclusion, the ground motion components have a more pronounced impact on bearing displacement than on bearing acceleration.

Figure 2: Contribution of a) the isolation system parameters; b) ground motions components

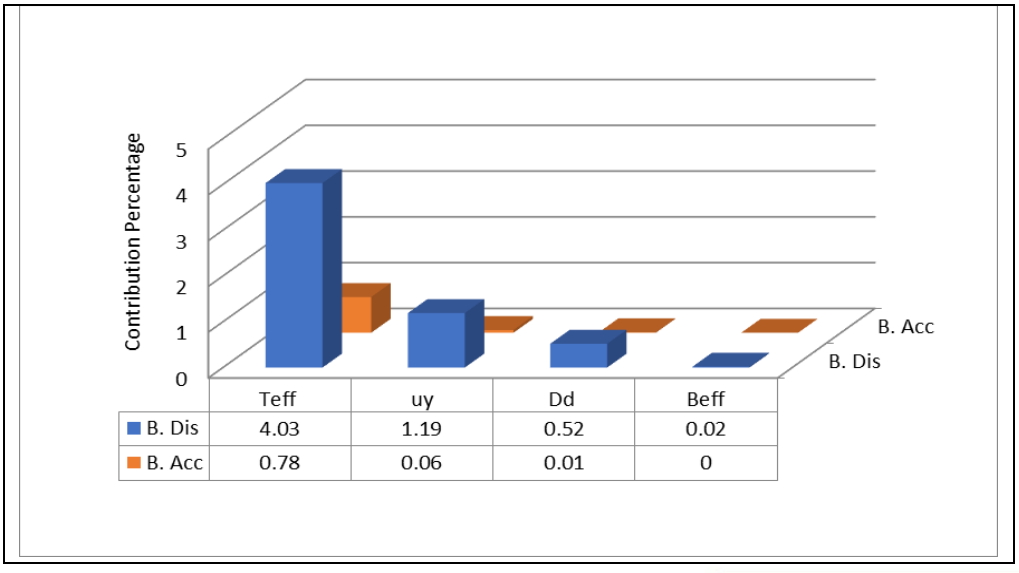

(A)

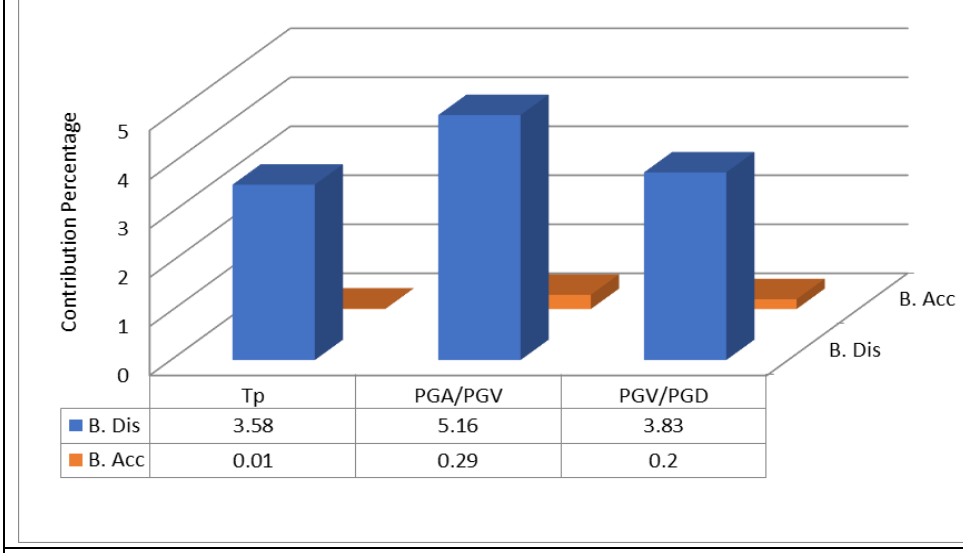

	Tp	PGA/PGV	PGV/PGD
B. Dis	3.58	5.16	3.83
B. Acc	0.01	0.29	0.2

(B)

6. Mechanical properties optimization

The desirability optimization process, introduced by Dodson et al. (Dodson et al., (2014)), is a widely used method for optimizing multiple responses. It employs an objective function called the desirability function, which ranges from zero outside the specified limits to one at the desired goal. The primary goal is to find a point in numerical optimization that maximizes the desirability function.

The concept behind this method is that a process with multiple quality characteristics is considered unacceptable if any of these characteristics fall outside the desired limits. Hence, the approach seeks operating conditions (x) that yield the most desirable response values. Each response, denoted as Yi(x), is assigned a desirability value (di(Yi)) between 0 and 1. A value of di(Yi) equal to 0 corresponds to an undesirable response, while a value of di(Yi) equal to 1 represents a desirable response. The shape of the desirability function for each response is determined by a weight, which influences the combination of individual desirabilities.

The overall desirability D (Eq. (2)) is obtained by combining the individual desirability values using the geometric mean. Figure 3 provides a graphical representation of the

desirability functions, where response desirability is one below the target and zero above the upper bound.

Figure 3: Graphical presentation of desirability diagram

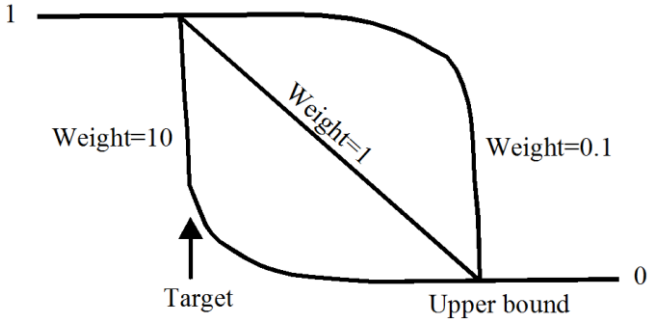

Eq. (2) will be used to measure overall desirability:

$$\mathbf{D} = (\mathbf{d_1}(\mathbf{Y_1}).\mathbf{d_2}(\mathbf{Y_2}) \dots \mathbf{d_k}(\mathbf{Y_k}))^{\frac{1}{k}} \quad (2)$$

In this equation, k is the number of responses.

The individual desirability function, denoted as $d_i(Y_i)$, may vary depending on the specific objective for each response. In cases where responses need to be minimized, the desirability function will be shaped differently compared to situations where responses should be maximized or assigned to a particular target value. This flexibility allows the desirability optimization process to cater to various optimization goals, tailoring the desirability function for each response accordingly.

The parameters are optimized using Minitab to minimize the bearing responses. Specific targets have been assigned for the isolator period, namely 2.5s, 3s, 3.5s, 4.0s, 4.5s, 5.0s, and 5.45s, while other parameters are adjusted to achieve minimal bearing responses. table 2 illustrates the optimized parameters corresponding to each target value, along with their respective desirability values. It is observed that for each target value of the isolator period, the yielding displacement and design displacement remain constant, while the effective damping ratio varies.

For instance, when the isolator period is 5.45 s, the effective damping ratio is found to be 6.05%. Conversely, for isolator periods of 3 s and 2.5 s, the damping ratio is 13.75%, indicating higher damping in those cases.

Based on table 2, the most favorable optimized values for the isolation system are achieved at the highest desirability value (D=0.99). Subsequently, these optimized parameters with higher desirability values are implemented to study the behavior of the low- and high-rise base-isolated buildings.

Table 2: Optimized value

Desirability value (D)	**0.9944**	**0.9931**	**0.9912**	**0.9889**	**0.9859**	**0.9821**	**0.9769**
Target value for (T_{eff} (s))	**5.45**	**5**	**4.5**	**4**	**3.5**	**3**	**2.5**
u_y (cm)	2.56	2.56	2.56	2.56	2.56	2.56	2.56
D_d (cm)	51.5	51.5	51.5	51.5	51.5	51.5	51.5
β_{eff} (%)	6.05	7.64	9.30	11.05	12.71	13.75	13.75

7. Optimized parameters on multi-degree of freedom models

In this section, we have examined the effectiveness of the optimized parameters of the isolation system on the MDOF model. This investigation was carried out using 126 pulse-like ground motions. Pulse-like ground motions are known for their higher intensity compared to non-pulse-like ground motions, resulting in lower and less destructive structural responses. Previous studies by Kohrangi, Vamvatsikos, & Bazzurro (2018) and Bagerzadeh Karimi (2019) have also supported this observation.

Consequently, the optimized parameters were found to be effective in mitigating structural responses under pulse-like ground motions. To conserve space and streamline the analysis, we have selected the two ground motions with the highest intensity as representatives among the entire set of selected ground motions.

To explore the optimal effectiveness of the chosen ground motions, their inherent components (PGA/PGV, PGV/PGD, and T_p) were taken into account, and the Analysis of Variance method (ANOVA) was employed. The findings indicate that bearing displacement is notably influenced by the lower limit of the PGA/PGV ratio and PGV/PGD ratio (when PGA/PGV is between 1 (1/s) and 6 (1/s), and PGV/PGD is between 0.05 (1/s) and 3 (1/s)). However, the pulse period does not exhibit a significant effect on bearing displacement.

Furthermore, the contribution percentage analysis of ground motion components, as depicted in Figure 2, highlighted the significant impact of the PGA/PGV ratio on bearing displacement. Therefore, two ground motions (RSN1120 and RSN723) were chosen based on their PGA/PGV ratio to assess the behavior of both 5- and 20-storey base-isolated buildings.

Figure 4 illustrates the responses of the storeys and the for the optimized parameters of the isolation system corresponding to different desirability values under the influence of Kobe (RSN1120) and Superstition Hills (RSN723) ground motions. The analysis was conducted for both 20-storey and 5-storey base-isolated buildings.

Figure 4: Storey responses for 20-storey seismically isolated buildings based on the optimized parameters for each desirability value: A) considering RSN1120 ground motion; B) considering RSN723 ground motion

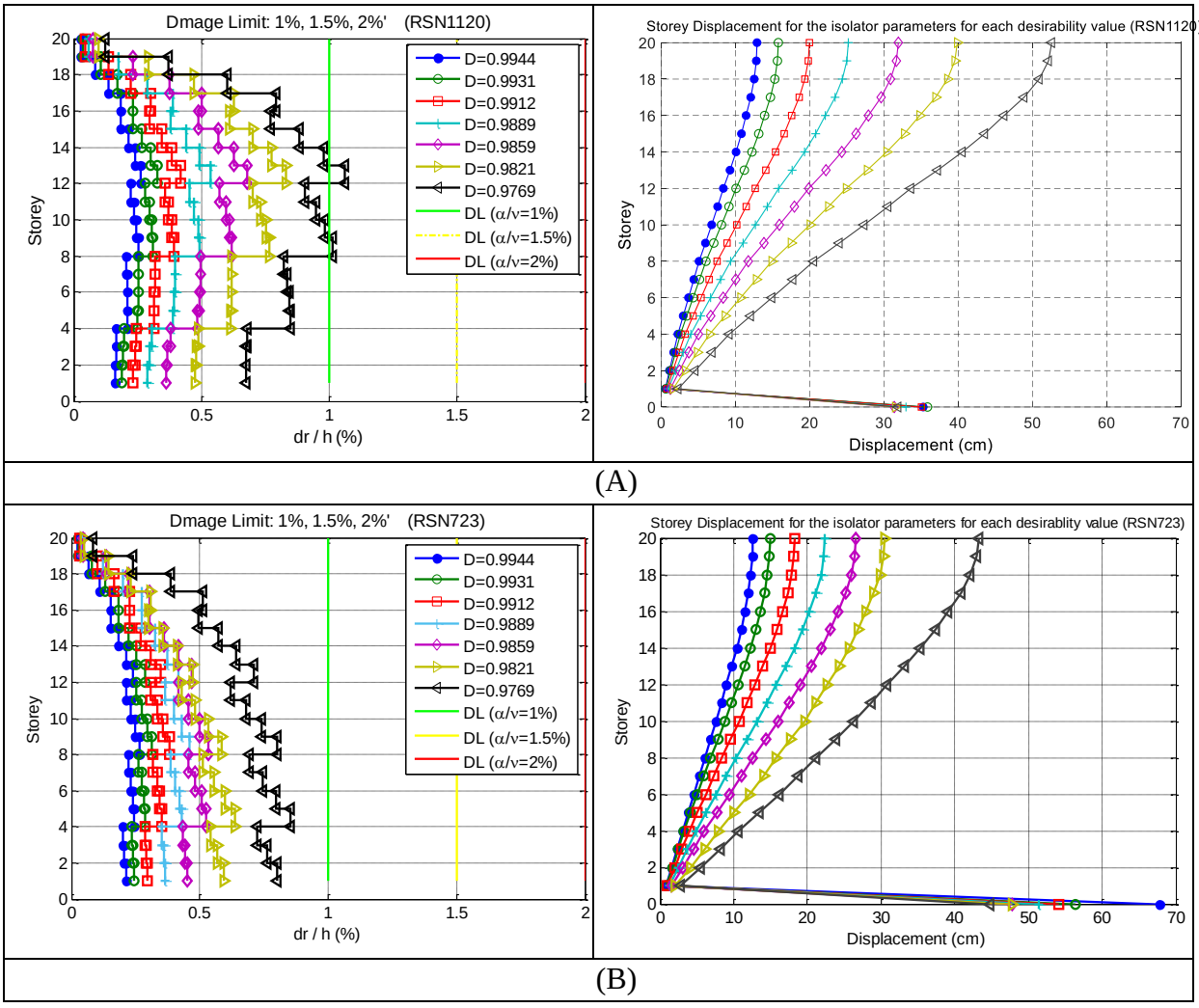

Based on the aforementioned findings, the optimized parameters with the highest desirability value (D=0.9944) demonstrate a remarkable reduction in responses for both 5- and 20-storey base-isolated buildings. To provide further insights, time history responses and floor responses have been presented, focusing solely on the optimized value with the highest desirability (Figure 5).

Figure 5: seismically isolated building responses for 20-Storey building considering A) KOBE ground motion (with RSN1120), and B) Northridge ground motion (with RSN1045)

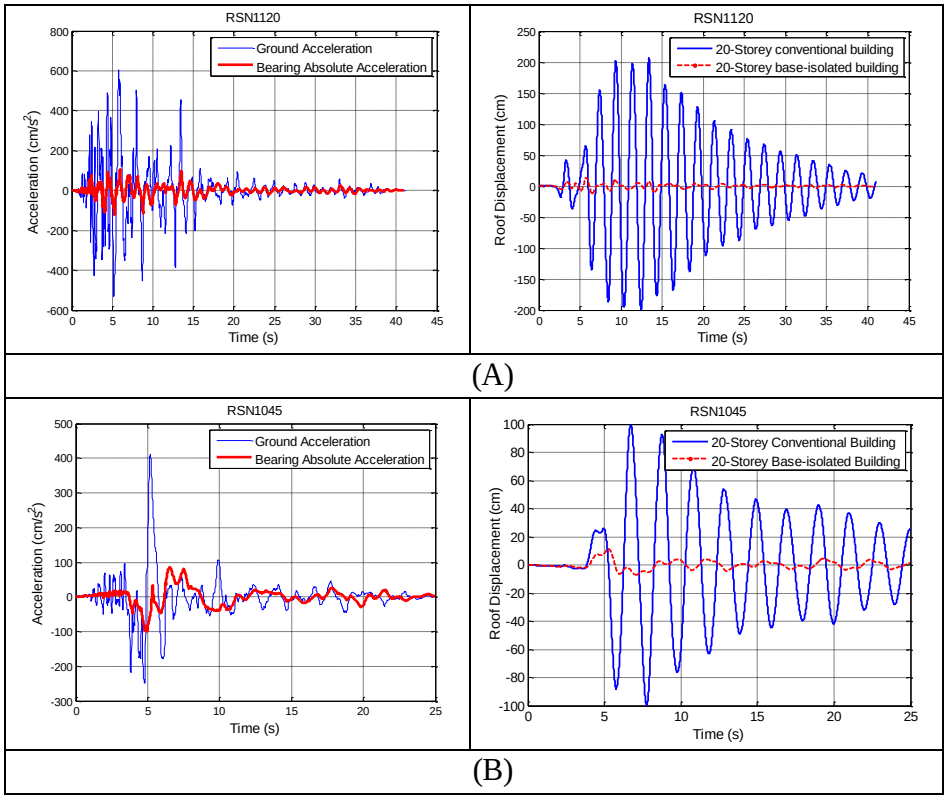

As it can be observed from figure 5, ground acceleration at the isolator level has significantly decreased, resulting in substantial reductions in top-floor responses. Additionally, the figure 5 exhibits storey displacement and acceleration, respectively, showing

8. Conclusions

In this study, a factorial modelling and optimization approach was applied to the mechanical properties of Lead Rubber Bearings (LRBs) in the context of variable pulse-like ground motions. The main objective was to minimize response quantities of interest at the base-isolation system level. The key findings of this research are as follows:

1) The period of isolation made the most significant contribution, accounting for approximately 4.03% of bearing displacement and 0.78% of bearing acceleration.

2) The ratio of PGA (Peak Ground Acceleration) to PGV (Peak Ground Velocity) had a substantial impact on bearing displacement, accounting for approximately 5.16%. Additionally, the PGV/PGD (Peak Ground Velocity/Peak Ground Displacement) ratio and pulse period contributed about 3.83% and 3.58% to bearing displacement, respectively. However, it was observed that ground motion components did not significantly influence bearing acceleration.

3) To enhance the performance of base-isolated buildings, the isolator parameters were optimized to minimize building responses, accounting for the diverse mass ranges of these structures. The study revealed that for the upper limit of the isolator period (5.45 seconds), the desirability value was approximately D=0.9944, closely approaching the ideal value of D=1. This optimization led to significantly reduced building responses when the isolator period was at its maximum and the effective damping ratio was at its minimum.

4) In conclusion, the optimized isolator parameters, achieving a desirability value of D=0.9944, were evaluated by examining both low-rise and high-rise base-isolated buildings. Remarkably, the building responses reached their minimum values when the upper limit of the isolator period (5.45 seconds) and the lower threshold of the damping ratio (6.05%) were taken into account.

References

Ahmadi, G. (1983). Stochastic earthquake response of structures on sliding foundation. *International Journal of Engineering Science, 2*(21), 93-102.

Alhan, C., & Gavin, H. (2005). Reliability of base-isolation for the protection of critical equipment from earthquake hazards. *Engineering Structures, 9*(27), 1435–49.

Alhan, C., & Öncü-Davas, S. (2016). Performance limits of seismically isolated buildings under near-field earthquakes. *Engineering Structures, 116*, 83-94. doi:https://doi.org/10.1016/j.engstruct.2016.02.043

Bagerzadeh Karimi, M. R. (2019). Seismic Performance Evaluation of the Base Isolation Systems (Thesis). 1-200. Eastern Mediterranean University.

Cheng, F., Jiang, H., & Lou, K. (2008). *Smart Structures Innovative Systems for Seismic Response Control.* Boca Raton, Florida: CRC Press Taylor & Francis Group. doi:https://doi.org/10.1201/9781420008173

Chimamphant, S., & Kasai, K. (2016). Comparative response and performance of base-isolated and fixed-base structures. *Earthquake engineering & structural dynamics, 45*(1), 5-27.

Dodson, B., Hammett, P., & Klerx, R. (2014). *Probabilistic design for optimization and robustness for engineers.* Wiley.

Elnashai, A., & Sarno, L. (2008). *Fundamentals of Earthquake Engineering*. Wiley & Sons.

Er, G. K., & Iu, V. P. (2000). Stochastic response of base-excited Coulomb oscillator. *Journal of Sound and Vibration*, 81-92.

Eurocode8. (1998-1.). *Eurocode 8, Design of structures for earthquake resistance- Part 1 : General rules, seismic actions and rules for buildings, EN.*

Greco, R., & Marano, G. (2016). Robust optimization of base isolation devices under uncertain parameters. *Journal of vibration and control, 22*(3), 853–68.

Jacob, C., Sepahvand, K., Matsagar, V., & Marburg, S. (2013). Stochastic seismic response of base-isolated buildings. *International Journal of Applied Mechanics, 1*(5), 1–21.

Jangid, R. (2000). Stochastic seismic response of structures isolated by rolling rods. *Engineering Structure, 8*(22), 937-46.

Jangid, R., & Datta, T. (1995). Performance of base-isolation systems for asymmetric building subject to random excitation. *Engineering Structure, 6*(17), 443-54.

Kodakkal, A., Saha, S. K., Sepahvand, K., Matsagar, V. A., Duddeck, F., & Marburg, S. (2019). Uncertainties in dynamic response of buildings with non-linear baseisolators. *Engineering Structures, 197.*

Kohrangi, M., Vamvatsikos, D., & Bazzurro, P. (2018). Pulse-like versus non-pulse-like ground motion records: Spectral shape comparisons and record selection strategies. *Earthquake Engineering & Structural Dynamics, 48*(1).